

See discussions, stats, and author profiles for this publication at: <https://www.researchgate.net/publication/228568820>

Modal Properties of Golf Club Wood Driver in Different Boundary Conditions

Article · January 2005

CITATIONS

0

READS

173

2 authors, including:



Bor-Tsuen Wang

National Pingtung University of Science and Technology

59 PUBLICATIONS 937 CITATIONS

SEE PROFILE

Modal Properties of Golf Club Wood Driver in Different Boundary Conditions

Bor-Tsuen Wang, Guo-Zhen Wu

Department of Mechanical Engineering

National Pingtung University of Science and Technology

E-mail: wangbt@mail.npust.edu.tw

ABSTRACT

This paper performs both theoretical and experimental modal analysis for a golf club wood driver in three kinds of boundary conditions, including free-free, free-grip and free-fixed. The finite element model of the golf club is constructed by using linear shell elements. Modal and harmonic response analyses are, respectively, carried out to obtain modal parameters and frequency response functions of the golf club. Conventional experimental modal analysis is performed to experimentally extract modal parameters, including natural frequencies, damping ratios and mode shapes. Results show that both FEA and EMA agree reasonably. Modal characteristics of the golf club in different boundary conditions are compared. The realistic boundary conditions of the grip can be well simulated and validated. The theoretical model can be useful for further analysis such as impact analysis.

Keywords: model verification, finite element analysis, experimental modal analysis, golf club wood driver.

1. INTRODUCTION

The golf is a popular sport now. The competition has been more intense on the golf court, so that the sport equipments are made more and more exquisite. The golf industry is also dedicated to the research of golf clubs. For example, the golf club wood driver was made by maple at first. Now, the golf club materials become the head titanium alloy head with carbon fiber shaft. The shooting range is increased from 200yards to about 400yards, such that the drive performance is much better than in the past. This also makes more attraction in golf tournament than ever.

Computer Aided engineering (CAE) is a commonly used method that will accelerate the golf club design and prototype development. Jones [1] used Computer Aided Design (CAD), Computer Measuring Machines (CMM) and Computer Numerically Controlled Machine (CNC) to develop models of various golf club types and introduced the progressive development of analytical method. Wang and Wu [2] theoretically studied vibration characteristics of golf club head and a whole golf club wood driver. The golf club in three types of boundary conditions, i.e. free, spring and fixed, was analyzed to compare their natural frequencies and mode shapes. When the spring constants at spring end approach to zero, the golf club acts just like that in the free boundary. On the contrary, for the spring constants approaching to

infinity, the modal characteristics of the golf club are similar to those of the fixed boundary. Xie [3] defined the geometry parameters of the golf club and explained the importance of these design variables. He established the procedure for the design of golf club head with CAD software. Finally, the sweet spot and strength of the golf club head were determined by the impact analysis.

Dynamic characteristics of the golf club are very interested and widely studied. Swider et al. [4] used finite element analysis (FEA) and experimental modal analysis (EMA) to analyze the modal properties of a golf club. The physical interpretations of mode shapes for the club head were described. Merkel and Tom [5] used the similar approach to analyze four clubs and compared their dynamic characteristics. Milne and Davis [6] used a high-speed video system to investigate the golf swing. The shaft model to study flexing behavior during swing was constructed, and the shaft strains were measured during the actual golf swing to verify the validity of dynamic model. Knight et al. [7] developed a measurement system that can obtain the shaft strain during the golf swing and characterize the dynamic performance of the golf club shaft. They developed a measurement-based procedure that would help to determine the optimum shaft for an individual golf player. Knight et al. [8] further built a virtual instrument utilizing the collected golf strain data and converting the data as the input to a machine that can behave like a human golf player. The machine can reproduce the resulting strain profile from the player.

The golf club performance in terms of the vibration index is of interest. Okubo and Simada [9] employed EMA and FEA to investigate the dynamic of the golf club for force identification of the head due to ball impact. The sweet spot was defined based on frequency response function (FRFs). The FRFs at the sweet spot appear relatively flat in comparison to those at other areas. Wang and Huang [10] discussed three types of golf clubs that have the same grip and shaft, but different heads. The vibration characteristics of the golf clubs were analyzed via FEA and EMA, respectively. They discussed the feasibility for the use of modal parameters, including natural frequencies, mode shapes and damping ratios, to define the club performance index. Hocknell et al. [11] obtained the experimental modal data from the non-contacting laser Doppler vibrometry and electronic speckle pattern interferometer, respectively and validated with the finite element model. Wang et al. [12] performed model verification of a carbon fiber golf shaft via FEA and EMA. Based on the experimentally determined

natural frequencies, optimum analysis was performed to predict the mechanical properties, includes Young's modulus and Poisson ratio. Friswell et al. [13] used the same approach to analyze the golf club and estimated stiffness of the shaft and the inertia properties of the golf club head.

This paper adopts FEA and EMA to perform model verification for the golf club in different kinds of boundary conditions. The vibration characteristics of golf club in different boundary conditions are discussed, respectively. The developed and validated finite element model can then be used for further analysis.

2. Finite Element Analysis

A typical golf club wood driver, OM136, is considered in this work. Figure 1 shows the geometry model and Table 1(a) 1(c) show the material and geometry properties for golf head, carbon fiber shaft and grip, respectively.

Finite element code, ANSYS, is employed to perform theoretical analysis in this work. The geometry model is established by using Pro/E. The four-node linear shell element (shell63) is used to model the golf club head and the shaft.

The golf club in different boundary conditions are considered and described as follows:

1. Free-Free boundary: Figure 2(a) shows the finite element model of golf club in free-free boundary condition. There are no displacement constraints at all.
2. Free-Grip boundary: Figure 2(b) shows the finite element model of golf club in free-grip boundary condition. The 3D linear and rotational spring elements (combin14) are used to simulate the grip boundary and located at those positions for handgrip. The linear and rotational spring constants are optimally determined through model verification and identified as $K_L = 2298.5 \text{ (N/m)}$ and $K_\theta = 90489 \text{ (N-m/rad)}$, respectively. The model can theoretically simulate the real grip condition.
3. Free-Fixed boundary: For the spring constants approaching to infinity, modal characteristics of the golf club are similar to those of the free-fixed boundary condition [2]. The linear and rotational spring constants are identified as $K_L = 0.25331 \times 10^6 \text{ (N/m)}$ and $K_\theta = 0.73791 \times 10^{13} \text{ (N-m/rad)}$, respectively. Figure 2(c) shows the finite element model. The spring elements are imposed at the clamped portion.

3. Experimental Modal Analysis

The experimental setup is shown in Figure 3. An impact hammer is used to excite the golf club wood driver. The response is measured by an accelerometer fixed at the corner on the hit-face of golf club head. The FFT Analyzer (SIGLAB) is used to record the frequency response functions between the measured acceleration and impact force. The general-purpose curve fitting

software, ME'Scope, is used to estimate the modal parameters, i.e. natural frequencies, damping ratios and mode shapes.

Figure 4(a) and 4(b) show the grid points for the head and shaft, respectively. Only the hit-face of golf head is grided for testing. The test points on the carbon fiber shaft are divided into two directions that are swing and droop, respectively, as shown in Figure 4.

There are three kinds of boundary conditions considered in experiments corresponding to the finite element model and described as follows:

1. Free-Free boundary: Figure 5(a) shows the experimental setup for the free boundary. The grip end is suspended by a nylon string to simulate free boundary. The golf club head is grided and marked up to 103 test points, and the club shaft is 100 points.
2. Free-Grip boundary: Figure 5(b) shows the experimental setup for the fixed boundary. The grip is gripped by human's hands to reveal the actual grip condition. The face on the head is grided only 6 test points, and the club is 22 points.
3. Free-Fixed boundary: Figure 5(c) shows the experimental setup for the grip boundary. The grip is clamped and fixed by the vise. The golf club head is grided and marked up to 103 test points, and the club shaft is 84 points.

This work adopts the test procedure, the roving hammer through all of the test points with the fixed accelerometer at the corner on the hit-face of golf head.

4. Results and Discussions

4.1 Finite Element Analysis

This section presents modal characteristics of the typically golf club wood driver in three kinds of boundary conditions using FEA. The physical interpretations of natural frequencies and mode shapes are generally discussed as follows:

1. For free-free boundary condition, there are six rigid-body modes; the first flexible-body mode starts at the 7th mode. The lowest natural frequency is about 32Hz. For free-grip and free-fixed boundaries, their lowest natural frequencies are about 2Hz and 5Hz, respectively.
2. The typical structural mode shapes of the golf club are tabulated in Table 3. There are bending modes in both swing and droop directions for the club as well as the expanding mode of the shaft. The golf club head reveals its surface modes, independent.
3. For grip and fixed boundaries, the golf club reveals torsional modes that are not observed in free boundary. This can be the cause of unbalance mass effect of the club head.
4. Above 1000Hz, i.e. the modes larger than the sixth bending mode, the club bending modes can be observed almost identical and corresponding to each others for all three boundary conditions.
5. The first typical surface mode of the golf club head as shown in Table 2 is the (1,1) mode on the hit-face of head. The natural frequencies of the (1,1) and (2,1) modes are about 4200Hz and 6200Hz, respectively.

The modal frequencies of the head surface modes are rarely effected due to boundary conditions.

4.2 Experimental Modal Analysis

The club in the three boundary conditions as described previously is also to perform EMA. The modal characteristics of the EMA results are summarized as follows:

1. For club shaft modes, only both swing and droop bending modes can be determined due to the test grid plan. The shaft-expanding mode cannot be obtained. Additionally, the torsional modes of the club are observed and can be due to the coupling effect of swing and droop motions.
2. The first flexible mode is 35Hz for Free-Free boundary condition and can be identified as the bending mode in swing direction. For grip and fixed boundaries, the first modes are about 14Hz and 29Hz, respectively, and reveal to be the torsional mode. This can be the cause for the unbalance effect of head mass in grip and fixed boundaries.
3. Most bending modes extracted from EMA are in the swing direction, because the accelerometer is fixed at the swing direction during EMA. Therefore, some bending modes in the droop direction are not clearly observed.
4. For the surface mode of club head, the same phenomena found in FEA can be observed in experiments. Both the (1,1) and (2,1) modes of the hit-face of head are 4300Hz and 6300Hz, respectively, and almost the same for all boundaries.

4.3 Model Verification Results

Figure 6 shows the procedures for model verification and design validation. In EMA, the actual structure is tested; therefore, the FE model is adjusted base on the experimental results. The mechanical properties of the club and the spring constants, as specified section 2, to present the boundary are adjusted accordingly to fit the experimental modal data. Finally, the equivalent FE models can be obtained, for the club in three different boundary conditions, respectively.

4.3.1 Verification of FRFs

Figures 7(a)-7(c) show the typical transfer FRFs for the three kinds of boundary conditions, respectively. For (i,j)=(12,141), the accelerometer is located at point 12 near the corner of the hit-face of head, and the hammer is applied at point 14 near the grip of the shaft. There are two curves in each plot. One is the experimental FRF and the other is the synthesized. That both curves agree reasonably indicate the success in curve-fitting process. As one can observe, there are over about 60 resonant modes in 10000Hz frequency range. It is noted that the first head surface mode is at 4200Hz. There appear quite similar FRFs above 4000Hz for all boundaries. As well be discussed later, the modal properties of the club in different boundary conditions above 4000Hz are rarely effected.

4.3.2 Verification of Natural Frequencies

Table 4 shows the comparison of natural frequencies

between theoretical and experimental results for three kinds of boundary conditions. Only those corresponding modes between EMA and FEA are shown. The symbol F represents the flexible body mode obtained from FEA, and the symbol E is from EMA. As one can observe from Table 4, the errors in free-free boundary condition are within 10%. Only a few modes which errors are greater than 10% for the grip and fixed boundaries. They are F-3, F-7 and F-13 for grip boundary, and F-12 and F-22 for fixed boundary. There appears reasonable fit of FE model in comparison to the golf club in realistic boundary conditions.

4.3.3 Verification of Mode Shapes

Table 5 shows the comparison of mode shapes between theoretical and experimental results for three kinds of boundary conditions, some observations are discussed as follow:

1. Free-Free boundary: Those from mode F-2 to mode F-29 are bending modes in the swing direction, and those from mode F-32 to F-35 are head surface modes. In particular, modes F-32 and F-51 reveal the (1,1) and (2,1) modes of the hit-face, respectively.
2. Free-Grip boundary: Mode F-3 is the torsional mode of the golf club due to the mass unbalance of the head. Those from mode F-9 to F-29 are bending mode in the swing direction, and those from F-39 to F-56 are head surface modes.
3. Free-Fixed boundary: There appear very similar characteristics as observed in free-grip boundary.

Generally speaking, both FEA and EMA reveal a reasonable agreement for mode shapes appearance in three kinds of boundary conditions. And, as discussed previously the natural frequency comparison are generally within $\pm 10\%$ error. The FE model of the golf club can be experimentally verified and useful for other analysis.

4.3.4 Verification of Damping Ratios

It is noted that damping ratios can not be determined theoretically. Table 6 tabulates the modal damping ratios from EMA for the three boundary conditions. The accumulative averaged damping ratios are also shown. As one can observe, the damping ratios in grip boundary reveal the largest, and those in fixed boundary are the next. Damping effect in free boundary is the smallest. The soft-grip boundary can result in large damping effect and easily dissipate the vibration due to impact. An experience golf player could generally take advantage of these phenomena to properly release the grip strength after swing.

4.4 Comparison of different boundary conditions

To further compare the modal characteristics of the golf club in three kinds of boundary conditions, Table 7 tabulates the natural frequencies for those the same or similar mode shape interpretation for different boundaries. Discussions are as follows:

1. In general, the bending mode in grip and fixed boundaries appears an order higher than that in free boundary. For example, symbol Y-4_(Y-5) denotes the 4th Y-bending in free boundary and 5th

Y-bending in grip and fixed boundaries.

2. From Wang and Wu [2], natural frequencies for spring end boundary were right between the free and fixed boundaries. In this work, however, natural frequencies in grip boundary may be lower or higher than those in free boundary, but definitely lower than those in fixed boundary. For actual swing simulation, the handgrip effect should be carefully considered in modeling.
3. Above 4000Hz, the modal properties are almost the same in terms of natural frequencies and mode shapes for all three boundaries. This explains the similarity of FRFs in high frequency range as shown in Figure 7.

5. Conclusions

This work adopts FEA and EMA to perform model verification on a typical golf club driver in three kinds of boundary conditions. Some conclusions are summarized as follows:

1. Modal parameters determined from FEA and EMA agrees reasonably and are well interpreted. The analytical FE model can be verified and useful for further analysis, such as impact analysis.
2. The soft-grip boundary can result in large damping effect and easily dissipate the vibration due to impact.
3. Above 4000Hz, the modal properties are exactly the same in terms of natural frequencies and mode shapes for all three boundary conditions. The effect of realistic grip boundary should be carefully accounted in 100 frequency range.
4. The carbon fiber shaft is assumed the isotropic property in this paper. That causes the errors of natural frequencies greater than 10%. A refined material model for the club shaft can be of interest.

6. ACKNOWLEDGEMENT

The authors would like to acknowledge the support of O-TA Precision Casting Company Limited for providing with golf clubs.

7. REFERENCES

- [1] Jones, R., 1990, "Computer Based Methods for the Design and Manufacture of Golf Clubs," *Proceedings of the First World Scientific Congress of Golf* 13th, pp. 282-285.
- [2] Wang, B. T., and Wu, G. Z., 2004, "Modal Analysis of Golf Club Wood Driver," *The 12th National Conference on the Society Sound and Vibration*, Taipei, A3-2. (In Chinese)
- [3] Xie, Y. Z., 1995, "To Summarize Computer Aided Engineering of the Golf Club Head," *Industry Material*, Vol. 104, pp. 114-126. (In Chinese)
- [4] Swider, P., Ferraris, G., and Vincent, B., 1994, "Theoretical and Experimental Dynamic Behavior of a Golf Club Made of Composite Material," *The international Journal of Analytical and Experimental Modal Analysis*, Vol. 9, pp. 57-69.

- [5] Merkel, R. C., and Tom, B., 1998, "Dynamic Characterization and Comparison of Golf Clubs," *Proceedings of the 17th International Modal Analysis Conference*, pp. 513-517.
- [6] Milne, R. D., and Davis, J. P., 1992, "The Role of the Shaft in the Golf Swing," *J. Biomechanics*, Vol. 25, No. 9, pp. 975-983.
- [7] Knight, C. E., Leonard, R. G., Wicks, A. L., and Blough, T., 1997, "A Study of the Dynamic of Golf Clubs," *Proceeding of the 15th International Modal Analysis Conference*, Vol.2, pp. 1752-1757.
- [8] Knight, C. E., Leonard, R. G., Neighbors, J., and Wicks, A. L., 1998, "Golf Swing 'Signatures' on a Mockup Ball-Striking Machine," *Proceedings of the 17th International Modal Analysis Conference*, Vol. 2, pp. 509-512.
- [9] Okubo, N., and Simada, M., 1990, "Application of CAE (Computer Aided Engineering) to Golf Club Dynamics," *Proceedings of the First World Scientific Congress of Golf* 9th-13th, pp. 270-273.
- [10] Wang, B. T., and Huang, J. J., 200, "Vibration Characteristics and Quality for Golf Clubs With Different Heads," *The 8th National Conference on the Society Sound and Vibration*, Pingtung, pp. 209-216. (In Chinese)
- [11] Hocknell, A., Mitchell, S. R., Jones, P., and Rothberg, S. J., 1998, "Hollow Golf Club Head Modal Characteristics: Determination and Impact Applications," *Experimental Mechanics*, Vol.38, pp. 140-146.
- [12] Wang, B. T., Hong, Y. T., and Liu, W. C., 2003, "Determination of Mechanical Properties for the Golf Club Shaft," *The 11th National Conference on the Society of Sound and Vibration*, Keelung, pp. 63-69. (In Chinese)
- [13] Friswell, M. I., Smart, M. G., and Mottershead, J. E., 1997, "Updating Finite Element Models of Golf Clubs," *Proceedings of the 15th International Modal Analysis Conference*, Vol. 1, pp. 155-161.

不同邊界高爾夫球木桿振動與模態特性探討

¹王栢村 ²吳國禎

¹國立屏東科技大學機械工程系教授

²國立屏東科技大學機械工程系碩士班研究生

E-mail: wangbt@mail.npust.edu.tw

摘要

本文旨在對不同握把處邊界高爾夫球木桿進行模型驗證，考慮三種不同握把處邊界，自由、手握與固定。首先建構與實際結構對應的有限元素模型並進行理論的模態分析，同時也對實際結構進行實驗模態測試，可分別得其模態參數，並利用所得之模態參數進行比較驗證，確認有限元素模型之正確性。其結果顯示，有限元素分析與實驗模態分析的結果相當吻合，此三種不同握把處邊界之高爾夫球木桿之模態特性可被確認。最後，並探討其邊界的差異對於高爾夫球木桿結構振動特性的影響，希望藉此了解實際握桿情形。

關鍵詞：有限元素分析、實驗模態分析、高爾夫球木桿。

Table 1. Material and Geometry Properties of Golf Club Wood Driver

(a) Gold Club Head

Young's Modulus (N/m^2)	1.1595×10^{11}
Poisson's Ratio	0.27014
Density (kg/m^3)	4730
Thickness (mm)	2.6

(b) Carbon Fiber Club

Total Length (mm)	1017
Young's Modulus (N/m^2)	1.7199×10^{10}
Poisson's Ratio	0.30554
Density (kg/m^3)	1545.7
Length of Club (mm)	817
Small Diameter of Club (mm)	4.3
Large Diameter of Club (mm)	12
Thickness (mm)	2

(c) Grip

Length of Grip (mm)	200
Large Diameter of Grip (mm)	16
Small Diameter of Grip (mm)	14
Density (kg/m^3)	2500
Thickness (mm)	4

Tale 2. Typical FEA mode shapes

Physical interpretations	Mode shape
Bending mode in swing	
Bending mode in swing	
Shaft expanding mode	
Mode of head	

Table 3. Typical EMA mode shapes

Physical interpretations	Mode shape
Bending mode in swing	
Bending mode in swing	
Shaft rotating mode	
Mode of head	



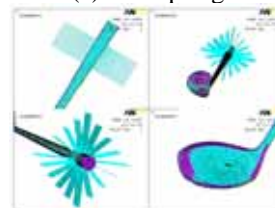
Figure 1. Geometry model of golf club



(a) free-free



(a) free-spring



(a) free-fixed

Figure 2. Finite element model (cont.)

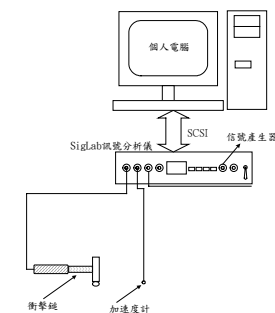
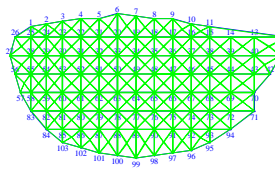
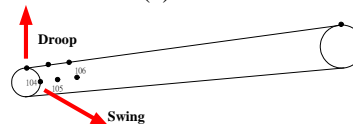


Figure 3. Experimental Setup



(a) Head



(b) Carbon fiber club

Figure 4. Points of experimental plan



(a) free-free



(b) free-grip



(c) free-fixed

Figure 5. Experimental setup

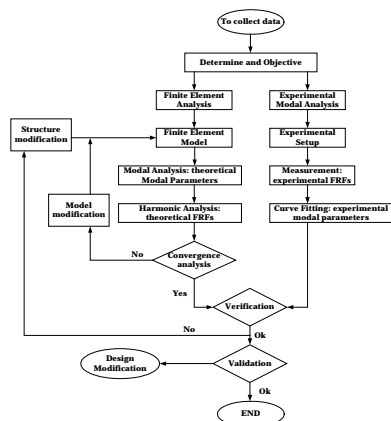
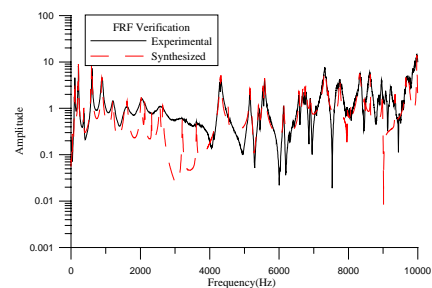
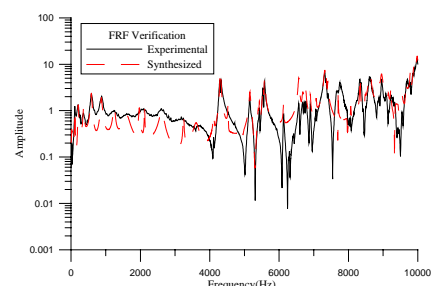


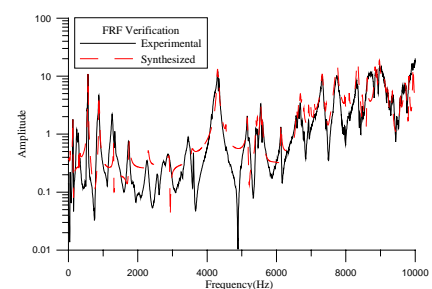
Figure 6. Verification and Validation



(a) free-free boundary



(b) free-grip boundary



(c) free-fixed boundary

Figure 7. FRF (i,j)=(i=12,j=141)

Table 4. Comparison of natural frequencies

Free-Free					Free-Grip					Free-Fixed				
Mode	Natural frequency	Mode	Natural frequency	Error (%)	Mode	Natural frequency	Mode	Natural frequency	Error (%)	Mode	Natural frequency	Mode	Natural frequency	Error (%)
F-2	35.794	E-1	35.7	-0.26	F-3	12.635	E-1	14.3	11.64	F-3	31.964	E-1	29.6	-7.99
F-4	108.21	E-4	109	0.72	F-7	127.41	E-3	112	-13.7	F-4	51.846	E-2	51.9	0.10
F-7	216.96	E-6	214	-1.38	F-10	200.33	E-4	207	3.22	F-5	58.979	E-3	59	0.04
F-9	388.58	E-8	368	-5.59	F-13	413.78	E-5	361	-14.6	F-6	128.21	E-4	126	-1.75
F-11	632.92	E-11	602	-5.14	F-15	639.35	E-6	584	-9.47	F-7	145	E-5	150	3.33
F-13	946.49	E-12	891	-6.23	F-18	957.37	E-7	873	-9.66	F-10	287.84	E-6	294	2.10
F-15	1315.7	E-13	1210	-8.74	F-20	1325.2	E-8	1240	-6.87	F-12	498.88	E-8	567	12.01
F-18	1727	E-15	1610	-7.27	F-23	1738.3	E-9	1600	-8.64	F-16	957.29	E-10	895	-6.96
F-20	2151.5	E-18	2320	7.26	F-25	2165.7	E-11	2120	-2.15	F-19	1184.7	E-11	1300	8.87
F-24	2612.7	E-20	2640	1.03	F-29	2625	E-12	2620	-0.19	F-22	1534.6	E-12	1750	12.31
F-26	3130.2	E-21	3210	2.49	F-31	3140	E-13	3240	3.08	F-26	2445	E-13	2300	-6.30
F-29	3701	E-22	3620	-2.24	F-34	3710	E-14	3610	-2.77	F-29	2959.4	E-14	2910	-1.70
F-32	4212.8	E-23	4300	2.03	F-37	4216.7	E-16	4300	1.93	F-34	3405	E-15	3550	4.08
F-35	4358.5	E-24	4320	-0.89	F-39	4342	E-17	4320	-0.50	F-37	4233.8	E-16	4300	1.54
F-36	4872.8	E-25	4530	-7.57	F-41	4885	E-18	4530	-7.83	F-39	4405.2	E-17	4330	-1.74
F-51	6230.2	E-33	6130	-1.63	F-56	6234.4	E-26	6130	-1.70	F-41	4945.6	E-18	4540	-8.93
										F-52	6156.9	E-24	6130	-0.44

Table 5. Comparison of mode shapes

Free-Free			Free-Grip			Free-Fixed		
Mode	FEA	EMA	Mode	FEA	EMA	Mode	FEA	EMA
F-2			F-3			F-3		
F-4			F-7			F-4		






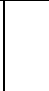





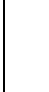

























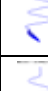


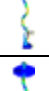




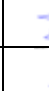
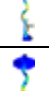







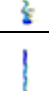




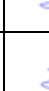
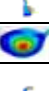

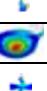












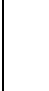

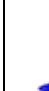









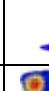
F-7			F-10			F-5		
F-9			F-13			F-6		
F-11			F-15			F-7		
F-13			F-18			F-10		
F-15			F-20			F-12		
F-18			F-23			F-16		
F-20			F-25			F-19		
F-24			F-29			F-22		
F-26			F-31			F-26		
F-29			F-34			F-29		
F-32			F-37			F-34		
F-35			F-39			F-37		
F-36			F-41			F-39		
F-51			F-56			F-41		
						F-52		
								

Table 6. Comparison of damping ratio

Free-Free			Free-Grip			Free-Fixed		
Mode	Damping ratio (%)	Average of accumulative total	Mode	Damping ratio (%)	Average of accumulative total	Mode	Damping ratio (%)	Average of accumulative total
1	6.66	6.66	1	26.4	26.4	1	8.54	8.54
2	1.16	3.91	2	23.4	24.9	2	2.66	5.6
3	2.47	3.19	3	4.61	14.755	3	1.6	3.6
4	1.9	2.545	4	4.23	9.4925	4	2.17	2.885
5	1.31	1.9275	5	3.91	6.70125	5	1.69	2.2875
6	1.08	1.50375	6	3	4.850625	6	0.372	1.32975
7	0.668	1.085875	7	2.43	3.640313	7	1.6	1.464875
8	0.763	0.924438	8	2.26	2.950156	8	0.529	0.996938
9	0.613	0.768719	9	5.51	4.230078	9	0.329	0.662969
10	0.33	0.549359	10	0.835	2.532539	10	0.781	0.721984
11	1.09	0.81968	11	0.277	1.40477	11	0.349	0.535492
12	1.39	1.10484	12	2.35	1.877385	12	0.854	0.694746
13	1.35	1.22742	13	0.334	1.105692	13	0.956	0.825373
14	1.45	1.33871	14	2.1	1.602846	14	0.767	0.796187
15	1.03	1.184355	15	0.358	0.980423	15	0.988	0.892093
16	0.817	1.000677	16	0.172	0.576212	16	0.351	0.621547
17	0.218	0.609339	17	0.263	0.419606	17	0.175	0.398273
18	0.083	0.346169	18	0.155	0.287303	18	0.177	0.287637
19	0.607	0.476585	19	0.251	0.269151	19	0.246	0.266818
20	0.368	0.422292	20	0.309	0.289076	20	0.221	0.243909
21	0.175	0.298646	21	0.499	0.394038	21	0.163	0.203455
22	0.151	0.224823	22	0.332	0.363019	22	0.25	0.226727
23	0.28	0.252412	23	0.159	0.261009	23	0.176	0.201364
24	0.219	0.235706	24	0.24	0.250505	24	0.168	0.184682
25	0.166	0.200853	25	0.223	0.236752	25	0.237	0.210841
26	0.225	0.212926	26	0.159	0.197876	26	0.153	0.18192
27	0.285	0.248963	27	0.28	0.238938	27	0.288	0.23496
28	0.187	0.217982	28	0.357	0.297969	28	0.205	0.21998
29	0.147	0.182491	29	0.206	0.251985	29	0.16	0.18999
30	0.199	0.190745	30	0.222	0.236992	30	0.145	0.167495
31	0.183	0.186873	31	0.157	0.196996	31	0.0727	0.120098
32	0.00037	0.093621	32	0.138	0.167498	32	0.0942	0.107149
33	0.157	0.125311	33	0.333	0.250249	33	0.381	0.244074
34	0.139	0.132155	34	0.0903	0.170275	34	0.115	0.179537
35	0.221	0.176578	35	0.126	0.148137	35	0.616	0.397769
36	0.165	0.170789	36	0.0275	0.087819	36	0.23	0.313884
37	0.175	0.172894	37	0.194	0.140909	37	0.11	0.211942
38	0.138	0.155447	38	0.0963	0.118605	38	0.1	0.155971
39	0.349	0.252224	39	0.086	0.102302	39	0.192	0.173986
40	0.0186	0.135412	40	0.154	0.128151	40	0.202	0.187993
41	0.172	0.153706	41	0.116	0.122076	41	0.102	0.144996
42	0.0722	0.112953	42	0.433	0.277538	42	0.0945	0.119748
43	0.0764	0.094676	43	0.517	0.397269	43	0.196	0.157874
44	0.337	0.215838	44	0.342	0.369634	44	0.0521	0.104987
45	0.0477	0.131769	45	0.151	0.260317	45	0.215	0.159994
46	0.013	0.072385	46	0.106	0.183159	46	0.432	0.295997
47	0.016	0.044192	47	0.21	0.196579	47	0.138	0.216998
48	0.0694	0.056796	48	0.128	0.16229	48	0.118	0.167499
49	0.0535	0.055148	49	0.128	0.145145	49	0.0839	0.1257
50	0.112	0.083574	50	0.128	0.136572	50	0.349	0.23735
51	0.248	0.165787	51	0.0809	0.108736	51	0.0655	0.151425
52	0.0357	0.100744	52	0.197	0.152868	52	0.091	0.121212
			53	0.267	0.209934			

Table 7. Comparison of physical interpretations of mode shapes

Free-Free		Free-Grip		Free-Fixed		Physical interpretations
Mode	Natural frequency (Hz)	Mode	Natural frequency (Hz)	Mode	Natural frequency (Hz)	
×	×	E-1	14.3	E-1	29.6	X-Torsion
×	×	×	×	E-2	51.9	Z-1_(Z-2)
E-1	35.7	×	×	E-3	59	Y-1_(Y-2)
×	×	×	×	E-4	126	Z-2_(Z-3)
E-4	109	E-3	112	E-5	150	Y-2_(Y-3)
E-6	214	E-4	207	E-6	294	Y-2_(Y-3)
E-8	368	E-5	361	E-8	567	Y-3_(Y-4)
E-11	602	E-6	584	E-10	895	Y-4_(Y-5)
E-12	891	E-7	873	E-11	1300	Y-5_(Y-6)
E-13	1210	E-8	1240	E-12	1750	Y-6_(Y-7)
E-15	1610	E-9	1600	E-13	2300	Y-7_(Y-8)
E-18	2320	E-11	2120	E-14	2910	Y-8_(Y-9)
E-20	2640	E-12	2620	E-15	3550	Y-9_(Y-10)
E-21	3210	E-13	3240	×	×	Y-10_(Y-11)
E-22	3620	E-14	3610	×	×	Y-11_(Y-12)
E-23	4300	E-16	4300	E-16	4300	(1,1)
E-24	4320	E-17	4320	E-17	4330	Y-12_(1,1)
E-25	4530	E-18	4530	E-18	4540	Y-13_(1,1)
E-33	6130	E-26	6130	E-24	6130	(2,1)